ISSN: 2395-1680 (ONLINE)
DOI: 10.21917/ijme.2019.0136

COMPACT AND BLOCKER-TOLERANT LOW-NOISE AMPLIFIER FOR SATELLITE RADIO

Chin Leong Lim
Avago Technologies, Malaysia

Abstract

Satellite Digital Audio Radio Service's (SDARS) reception over 2320-2345MHz can be blocked by cellular transmissions in the neighbouring bands. In vehicles, the blocking is exacerbated by SDARS sharing a common radome with cellular aerials. Considering the SDARS satellites are ~40,000km away, this is an extreme example of the near-far problem. Among cellular services, the Wireless Communications Service's (WCS) 2305-2320MHz and 2345-2360MHz bands are the most disruptive because they sandwich SDARS without any guard band. As SDARS aerial on the car roof is connected to the receiver through a long coaxial cable, an outboard low noise amplifier (LNA) is necessary to overcome cable loss. A compact LNA is required because of the small radome. Conventionally, a band-select filter before the LNA (pre-filter), is used to defend against blockers, but the filter's insertion loss can significantly degrade the overall noise figure. Furthermore, the space constraint necessitates a miniature filter which accentuates the loss. To reject WCS, the filter must possess narrow fractional bandwidth (~1%) and steep skirts. To reduce component count, we integrated amplifiers, biasing, impedance matching and filters into a 5×5mm^2 multi-chip on board (MCOB) module. The conflicting requirements for low noise and blocking immunity are satisfied by relocating the filter to mid-LNA. In conclusion, this design achieves previously unattainable miniaturization and blocking performance.

Keywords:

Satellite Digital Audio Radio Service Low Noise Amplifier, Blocker Tolerant, Cellular Coexistence, Miniaturize

1. INTRODUCTION

The 2320 to 2345MHz band is licensed to Sirius XM in US and Canada for broadcasting Satellite Digital Audio Radio Service (SDARS) compact disc quality audio to paying subscribers [1] [2]. Although cellular transmissions are on different frequencies, they can disrupt SDARS reception through blocking (Fig.1). The blocker can either emanate from nearby vehicles, or can be self-inflicted because the vehicular SDARS aerial often share a common radome with cellular aerials [3] [4] [5] where the unwanted coupling is typically less than -20dB [6]. Considering the SDARS satellites are ~40,000km away, this is an extreme example of the near-far problem. Although all existing cellular bands can block SDARS to some degree, the proposed Wireless Communications Service (WCS) in the 2305-2320MHz and 2345-2360MHz bands is the most potentially disruptive because the two bands sandwich SDARS without any guard band [7] [8].

For vehicular SDARS, the roof-top radome is connected to the dash-mounted receiver through 15-20 feet of coaxial cable [9]. Therefore, an outboard low noise amplifier (LNA) is required to overcome cable loss [10]. To achieve good noise performances, most of the prior arts realized the LNA with discrete transistors (Table.3). However, discrete implementations suffer from high component count and large printed circuit board (PCB) area and so, are incompatible with the small radome dictated by the car's aesthetic and aerodynamic considerations [11].

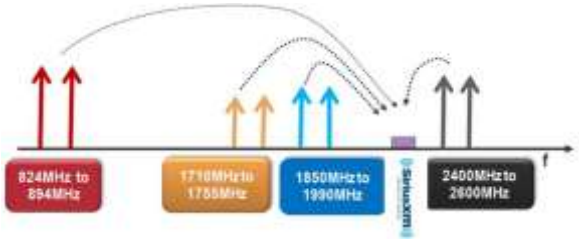

Fig.1. The SDARS band allocated to Sirius XM is surrounded by cellular services. Nearby cellular transmissions can impair the weak-signal SDARS reception

Narrowband receivers conventionally employ a band-select filter before the LNA (pre-filter) as the primary defence against out-of-band (OOB) blockers [12]-[14]. Since there is no gain before the pre-filter, its insertion loss will directly add to the overall noise figure (NF). Space constraint inside the fist-size radome necessitates a miniature microwave filter (<4mm^2) in this slot, but such tiny filters have substantial insertion loss [15] that will raise the NF above the acceptable threshold (<1.1dB). If the band-select filter is relocated to the middle of the LNA chain, i.e. an inter-stage filter, the NF degradation due to filter loss can be prevented. On the flip side, without the pre-filter, the first RF stage is exposed to OOB blockers. Hence, sensitivity and blocking immunity are conflicting requirements in the SDARS LNA.

In existing designs, the inter-stage filter is implemented using either surface acoustic wave (SAW) or dielectric filter technology but the off chip filter adds PCB space and cost. To reject WCS interferences, the filter's fractional bandwidth will need to be ~1%, but it is challenging to meet this requirement in a miniature microwave filter. Due to the lack of microwave filters that are compact, low-loss and narrowband, previous designs are incapable of rejecting WCS interferences (Table.3).

Blocking impairs reception by raising NF via either one or both of the following mechanisms: (a) the LNA's gain compresses and this allows pre-existing noise to dominate, or (b) the low frequency noise is up-converted by mixing with the interference [16]. The SDARS LNA will likely encounter persistent mobile phone use (e.g. navigation apps) in the same vehicle but the LNA prior arts did not report their blocking performances.

To reduce SDARS LNA's cost and size, we integrated RF amplifiers, active biasing, impedance matching and band-select filtering into a miniature multi-chip on board (MCOB) module. To resolve the conflicting requirements for low noise and high blocking immunity, we adopted inter-stage filtering and distributed the LNA gain to mitigate blocking. To fill the void on SDARS LNAs' blocking performance, this parameter is reported

for the first time. This article summarizes the design considerations and key performances.

2. MATERIAL AND METHOD

The outboard SDARS LNA sits between two sub-optimal components: (i) an omnidirectional or all-sky aerial with an attendant low gain – typically ≤4dBi [17] [18], and, (ii) a long cable run of around -10dB loss. To compensate for the gain shortfall, the LNA needs to provide ~35dB of gain. To this end, a high-gain semiconductor process is desirable because it can minimize the number of amplifier stages required. The chosen process - 0.25μm enhancement-mode pseudomorphic high electron mobility transistors (ePHEMT) [19] [20] is decided upon after weighing performance and cost considerations. Previously, this process has enjoyed commercial success in cellular base-stations' amplifier applications [21]-[24].

To achieve the target gain with the fewest stages, the cascode configuration will be used wherever possible. Using this process, the target gain can be achieved using three amplifier stages, Q_1-Q_3 (Fig.2). However, the 1st stage uses common source because it has better noise and blocking performances, while the next two stages are cascode for their higher gain. To minimize both development time and risks, Q_1-Q_3 are not developed from scratch but are borrowed from existing commercially-available monolithic microwave integrated circuits (MMICs) [25] [26]. The overall gain and NF distribution is given in Table.1.

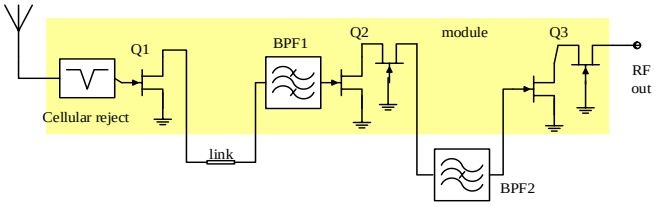

Fig.2. The miniature module (yellow area) integrates the LNA's core components consisting of three amplifiers Q1-3 and band-pass filter BPF1

Table.1. Target gain/loss and noise figure for each stage

	Connector and input trace	Q_1 amp.	BPF_1 filter	Q_2 amp.	BPF_2 filter	Q_3 amp.	Total
G(dB)	-0.1	10.1	-1	13.3	-3	16.4	35.7
NF(dB)	0.1	0.8	1	0.84	3	0.83	1.1

2.1 GAIN DISTRIBUTION FOR BLOCKER TOLERANCE

The second and third LNA stages, $Q_{2\text{-}3}$, are protected from OOB blockers by the inter-stage filters, $BPF_{1\text{-}2}$. In contrast, the first stage Q_1 has no protection from blockers because of the decision to forgo band-select pre-filtering in the interest of noise performance. Hence, Q_1 is the bottleneck for blocking performance. To mitigate Q_1's blocking vulnerability, the stage gain is deliberately kept low (~10dB) because this has the effect of raising the input gain compression point (IP1dB). Although it is also possible to improve blocking immunity by raising the bias current, this option is constrained by the 100mA current limit mandated by the service provider (Sirius). For improved rejection at cellular frequencies, Q_1's input network also incorporates notch filters at 860MHz and 1960MHz.

Since Q_2 and Q_3 are preceded by filters, they can have higher gains without the risk of blocking. Their higher gains are achieved by using cascode stages as opposed to Q_1's common-source topology.

While low-to-high gain distribution between $Q_{1\text{-}3}$ improves blocking tolerance, it sacrifices NF because the first stage gain is insufficient to overcome the subsequent stages' noise contribution. As a result, the overall noise Fig.is ~0.3dB higher than the first stage's (Table.1). However, this amount of NF degradation is significantly less than what the pre-filter would have incurred.

2.2 FILTER DISTRIBUTION FOR LOW NOISE

As discussed previously, the filters' positions in the LNA chain represent a compromise between blocker rejection and noise performances. To circumvent the unavailability of a tiny filter with the combination of low loss and narrow bandwidth, the filtering function is spread over two locations. The 1st filter BPF_1 is internally connected between Q_1 and Q_2. Due to Q_1's low gain, BPF_1 must have low insertion loss in order to preserve the overall noise figure. Additionally, BPF1 must be sufficiently tiny to allow integration into the module. Film Bulk Acoustic Resonator (FBAR) technology [27]-[29] is selected for BPF_1 because it has a low insertion loss (~1dB) that belies its integration-ready 0.9×0.7mm^2 area [30]. However, its 75MHz bandwidth is sufficient to guard against existing cellular bands but not the planned WCS ones (Fig.4).

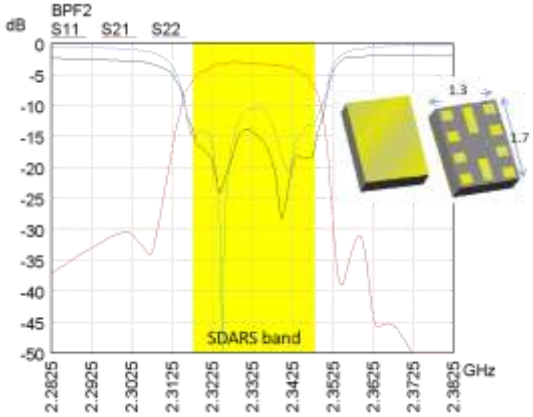

Fig.3. The 2nd bandpass filter (BPF2) is made with BAW technology and has enough selectivity to reject interferers from the adjacent WCS bands. However, it could not be integrated due to its large size (1.7×1.3×0.5mm^3) and so is implemented off-chip. Its 3dB in-band loss is significantly worse than that of BPF1

To enable coexistence with WCS, a second filter (BPF2) with the required selectivity, i.e. 25MHz bandwidth at the -3dB points, is connected externally between Q_2 and Q_3. This bulk acoustic wave (BAW) filter measures 1.7×1.3×0.5mm^3 [31] and is too large to integrate (Fig.3). It has substantially more loss than the first filter (3dB vs. 1dB), but this is an acceptable trade-off because the position between Q_2 and Q_3 has a lesser impact on the overall noise figure.

Another benefit of using two filters instead of one is improved stopband suppression. When BPF2 is evaluated alone, its upper stopband has a -40dB flyback (Fig.4). But when both filters are used, the flyback improves to better than -60dB.

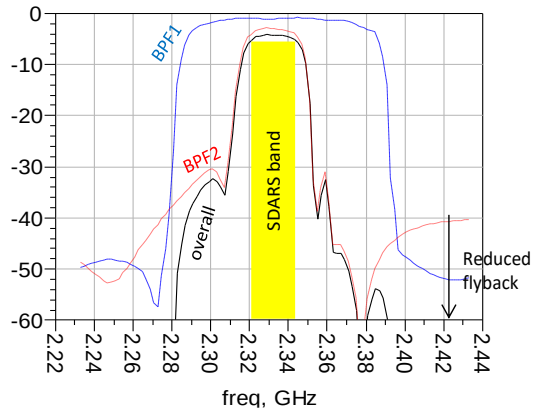

Fig.4. Simulated frequency responses of filters BPF1 (blue trace) and BPF2 (red) individually and when combined together (black). The combined response is steep enough to reject the adjacent WCS bands. It also beneficially solves BPF2's out-of-band flyback problem

2.3 MODULE FABRICATION AND PACKAGING

The module houses 3 chips for the amplifier stages ($Q_{1\text{-}3}$), 1 FBAR filter (BPF_1) and 21 passive components (Fig.5). After the components are mounted on the printed circuit board (PCB), the top side is over-molded with epoxy to achieve a final dimension of 5.0×5.0×0.95mm^3. The packaged device has 32 pins along its 4 edges. Four pads around the centre provide both low-inductance grounding and thermal paths.

2.4 PROTOTYPE FABRICATION

The evaluation fixture is intended to replicate the target application; i.e. an outboard SDARS LNA. For the fixture's PCB substrate, Rogers RO4350 [32] was selected after considering cost, performance and ease of fabrication. The module and off-chip components are surface mounted on one-side of the 10-mil PCB and the opposite side is used as the ground-plane (Fig.6). A FR4 backing layer is attached to the ground-plane side for rigidity and to increase the stack height to a standard 1.6mm. The PCB measures 38×23mm^2 but only ~140 mm^2 (or 16% of total area) is occupied by components. Edge-launched SMA receptacles provide connections for RF performance evaluation.

2.5 DESIGN VALIDATION AND TEST SETUP

The LNA module is designed to operate from a single 5V supply. The current consumption of each amplifier can be individually adjusted via off-chip resistances mounted on the evaluation fixture. This allows the current consumption to be traded-off for blocking immunity and vice-versa. In this prototype, $Q_{1\text{-}3}$'s quiescent currents are set to 47mA, 12 mA and 37mA, respectively because it optimizes blocking tolerance while remaining below the mandated 100mA current limit.

In addition to the experimental validation, the linear RF characteristics such as gain, NF and input or output matching are also simulated. The simulation's equivalent circuit model uses s-parameters supplied by the component manufacturers.

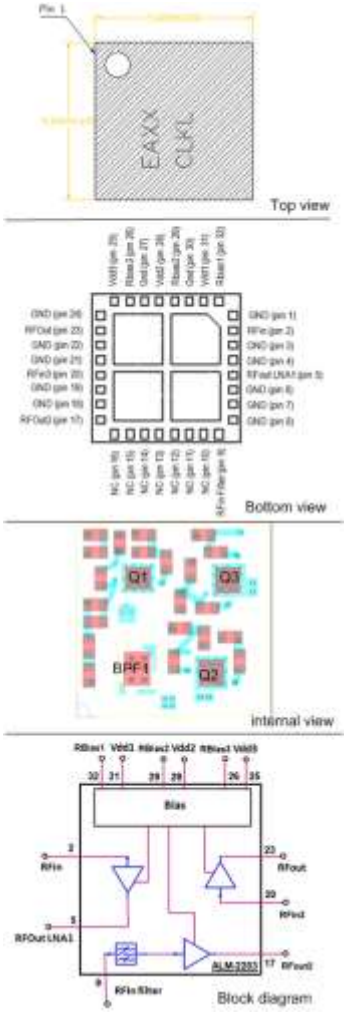

Fig.5. Module's mechanical, layout and functional details

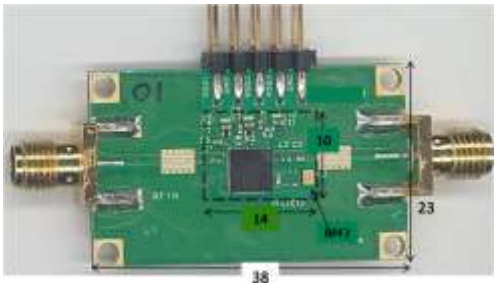

Fig.6. Assembled SDARS LNA. The component occupied area (enclosed by dashed rectangle) is only ~140mm^2 on the 38×23mm^2 printed circuit board

3. RESULTS

The experimental sample achieves state-of-the-art results for RF performances and miniaturization. This section first reports the general RF performances, followed by the blocking performance and finally, the miniaturization results.

3.1 GENERAL RF PERFORMANCES

This design has the noise, gain and selectivity performances to suit the SDARS LNA slot. The in-band NF of four samples averages ~1.0dB (Fig.7). The modeled NF shows a similar trend to the experimental result and the error is less than a few tenth of a dB.

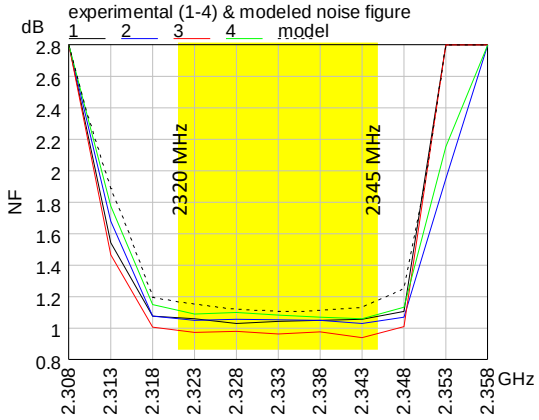

Fig.7. Inside the SDARS passband, the experimental noise figure averages ~1dB (n = 4)

In the SDARS band, the four samples have ~36dB gain (Fig.8). The modeled gain has the same behaviour as the experimental result, but has 2-3dB amplitude error.

The samples' in-band gain variation is <3dB. The ~2dB ripple in the passband is an unavoidable consequence of the high Q filter. The bandwidth at the -3dB points is ~30MHz. The WCS mid-band frequencies of 2313MHz and 2353MHz are suppressed by -11dBc and -16dBc, respectively. To our knowledge, this is the first and only SDARS LNA that is capable of rejecting WCS interference (Table.3).

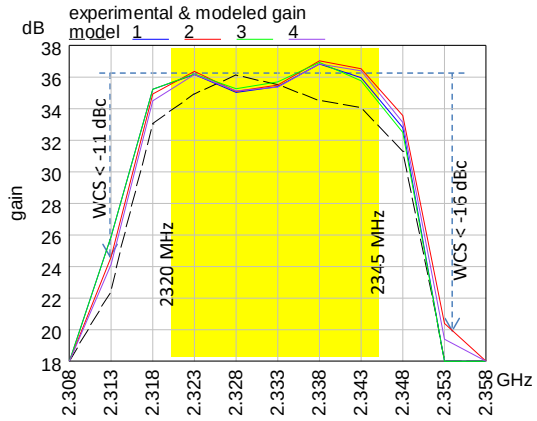

Fig.8. Inside the SDARS passband, the experimental gain averages ~36dB (n=4). WCS interferers on either sides of the SDARS band are suppressed by -11dBc and -16dBc, respectively

The LNA input provides a good match to the SDARS aerial for efficient transfer of signal energy. The experimental inband input return loss (IRL) is better than -14dB (Fig.9). The model predicted a poorer return loss with a maximum error of ~10dB.

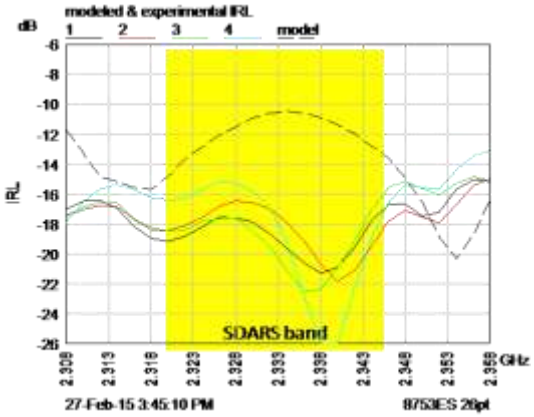

Fig.9. The experimental input return loss is better than -14dB inband. This good match can minimize loss between aerial and LNA

The LNA output can be connected to the receiver via a long run of coaxial cable without incurring excessive mismatch loss. Within the SDARS band, the experimental output return loss (ORL) is better than -9dB (Fig.10). The model erroneously predicts a better ORL and has a maximum error of 17dB inband.

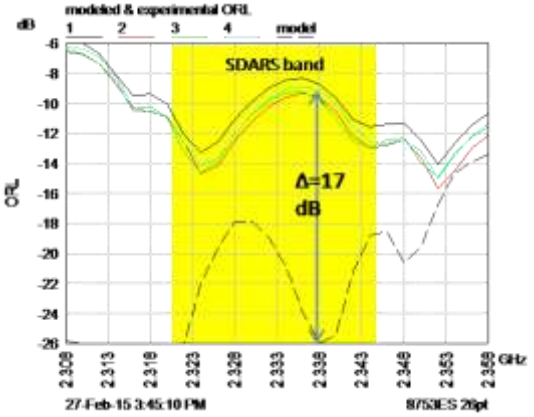

Fig.10. The experimental output return loss is better than -9dB, thereby minimizing mismatch loss in the interconnecting coaxial cable

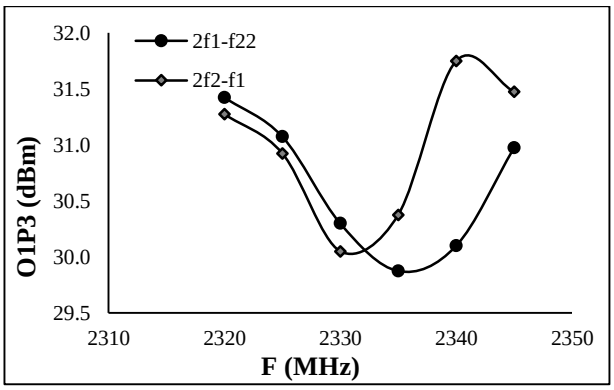

Fig.11. The experimental output third order intercept point (OIP3) exceeds 29.9dBm, thereby minimizing generation of spurious signals

This design is well suited to the crowded RF environment that an SDARS LNA is expected to perform in because its high linearity can minimize spurious reception. Its output third-order intercept point exceeds 29.9dBm; -5dBm if referenced to the input (Fig.11).

This design can handle substantial overdrive without going into gain compression. The experimental output power at 1dB gain compression (P1dB) exceeds 20dBm; or -14.8dBm, referenced to input (Fig.12). This is the highest P1dB ever reported for an SDARS LNA (Table.3).

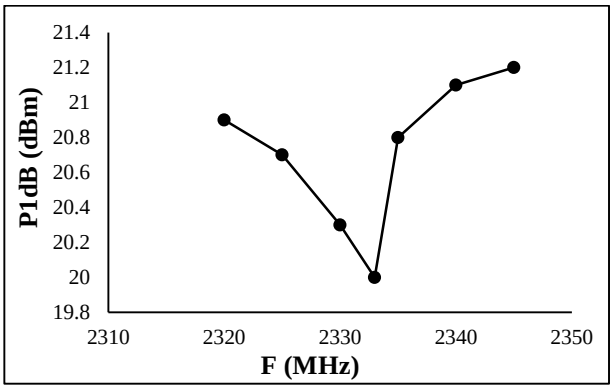

Fig.12. The >20dBm power at 1dB gain compression (P1dB) is the highest reported among SDARS LNAs

3.2 BLOCKING TOLERANCE

This design can withstand out-of-band (OOB) interference up to 0dBm without NF degradation. Using the measurement setup described in [33], the NF at the middle of the SDARS band (2333MHz) is monitored while a strong OOB signal is injected into the LNA input. The NF is more susceptible to the 2405MHz interferer than other evaluated frequencies (Fig.13), because of its proximity to the SDARS band. Conversely, the 1990MHz interferer impairs NF the least because it is attenuated by the notch filter preceding Q_1. To our knowledge, this is the first time an SDARS LNA's blocking performance is reported.

Different techniques have been proposed to boost blocking immunity in the absence of pre-filtering, but this work is arguably the most effective. This work is compared with designs from the cellular domain because blocking data from SDARS prior arts are unavailable. The comparison is based on the common metric for blocking: the amount of NF impairment (ΔNF) when subjected to a 0dBm blocker. At this power level, this work's worst case NF impairment is 0.1dB only, but the competition is impaired by 2.2dB to 9.8dB (Table.2). Another benefit of this work is that it is simpler (require fewer active components) than the competing blocker mitigating techniques.

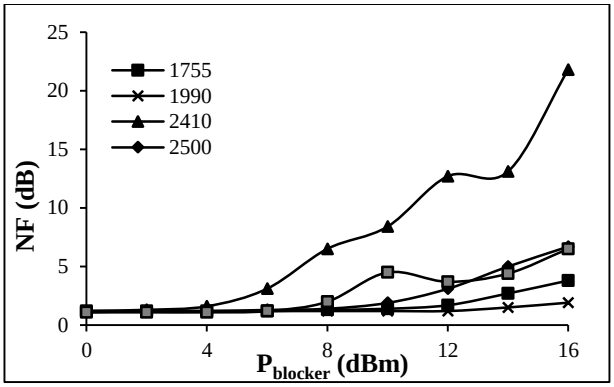

Fig.13. Experimental noise figure (*NF*) vs. blocker power (Pblocker) as a function of blocker frequency. NF is not impaired by any blocking power less than 0dBm. This level of blocking immunity is unprecedented (Table.2)

Table.2. Least noise figure impairment (Δ*NF*) among blocker mitigation schemes

Reference	Frequency (GHz)	NF (dB)	NF at 0dBm blocker (dB)	ΔNF (dB)
Noise-cancelling LNA and voltage sampling mixer [34]	2	3.2	13	9.8
Switched-capacitor N-path filter [35]	1.9	3.1	11.4	8.3
SAW-less narrowband [36]	1.9	2.9	8	5.1
Frequency-translational noise-cancelling [37]	2	1.9	4.1	2.2
Transformer-based LNA and transimpedance amplifier with 2nd order filter [38]	2	3.1	7.9	4.8
This work	2.3	1.1	1.2	0.1

3.3 MINIATURIZATION AND FUNCTION INTEGRATION

This design is smaller and integrates more functions than competing SDARS LNAs. This design's total PCB area of 874mm^2 is used in the size comparison (Table.3), even though the populated area is only 140mm^2. Nevertheless, it is 27% smaller than the next smallest competitor at 1200mm^2. It is also the only design with integrated matching and filtering.

Table.3. A smallest (PCB area) and most integrated (no. of functions) among SDARS LNAs. Additionally, it is the only design providing capable of rejecting the adjacent WCS bands (rightmost two columns)

Reference	Process Technology	Integrated functions			Components	PCB area (mm)	Noise figure (dB)	Gain (dB)	P1dB (dBm)	IIP3 (dBm)	WCS 2313 MHz suppression (dBc)	WCS 2353 MHz suppression (dBc)
		Active Bias	Matching	Filter								
Marino [39]	HJ-FET discrete	-	-	-	n.a.	n.a.	0.6	44	n.a.	n.a.	0	0
Xue [39]	-	-	-	-	n.a.	n.a.	0.8	32	n.a.	n.a.	0	0
CEL [40]	GaAs MMIC	Y	-	-	8	n.a.	1.8	27	n.a.	1.5	0	0
Sharawi [41]	ePHEMT discrete	-	-	-	n.a.	1798	0.9	26.8	n.a.	-4	0	0
Hong [42]	ePHEMT discrete	-	-	-	14	1750	0.9	30.3	n.a.	n.a.	0	0
Schwingschakl [43]	SiGe discrete	-	-	-	n.a.	n.a.	0.8	35	10	0	0	0
NXP [44]	SiGe discrete	-	-	-	28	1200	0.8	33	17	-5.2	0	0
Skywork [45]	GaAs pHEMT MMIC	Y	-	-	34	n.a.	0.6	32	17	-2	0	0
This work	ePHEMT MMIC	Y	Y	Y	14	874	1	35.4	20	-5	-13	-18

3.4 COMMERCIAL ADOPTION

This design been adopted by at least half a dozen manufacturers of SDARS receiving equipment. One example of a commercial product that has adopted this module is shown in Fig.14.

Fig.14. A commercially available SDARS LNA utilizing this design

4. CONCLUSION

The SDARS LNA's size and component count can be significantly reduced by integrating RF amplifiers, active biasing, impedance matching and filtering into a multi-chip-on-board module. The resultant LNA is significantly smaller than the prior arts but yet outperforms them in selectivity, gain compression and blocking immunity. Noise Figure degradation due to pre-filtering can be avoided by relocating the filter to a mid-LNA position. The absence of pre-filtering exposes the 1st stage to out-of-band blockers, but the ill-effects can be mitigated by redistributing the gain to later stages. Despite the simplicity, this technique results in better blocking tolerance than more complicated techniques. Although this work targets SDARS, the described blocker mitigation technique is readily adaptable to other wireless services.

REFERENCES

[1] Federal Communications Commission, "Satellite Digital Audio Radio Service", Available at: http://transition.fcc.gov/ib/sd/ssr/sdars.html, Accessed on 2018.

[2] K. Raghunandan, "*Satellite Digital Audio Radio Service System Architecture and Receiver Review",* Available at: http://www.ewh.ieee.org/r1/njcoast/events/RaghuNJcoast_2005.pdf, Accessed on 2005.

[3] J.F. Hopf, L.M. Reiter and S.M. Lindenmeier, "Compact Multi-Antenna System for Cars with Electrically Invisible Phone Antennas for SDARS Frequencies", *Proceedings of 2nd International ITG Conference on Antennas*, pp. 171-175, 2007.

[4] W.L. Stutzman and G.A. Thiele, "*Antenna Theory and Design*", Wiley, 2012.

[5] Laird, "Laird Technologies Introduces New Shark Fin Style Modular Antenna Assembly for Automotive Market", Available at: https://www.laird.com/node/580, Accessed on 2009.

[6] J. Kammerer, L. Reiter and S. Lindenmeier, "Automotive Hexband Antenna for AM/FM/GPS/SDARS and AMPS/PCS1900 Cell Phone in an only 65mm High Housing", *Proceedings of IEEE International Conference on Radio and Antenna*, pp. 111-117, 2012

[7] T.S. Rappaport, S. Di Pierro and R. Akturan, "Analysis and Simulation of Adjacent Service Interference to Vehicle-Equipped Digital Wireless Receivers from Cellular Mobile Terminals", *Proceedings of IEEE 72nd International Conference on Vehicular Technology*, pp. 1-5, 2010.

[8] J. Krauss, "The SDARS-WCS Mess", Available at: http://www.cedmagazine.com/articles/2010/06/capital-currents-the-sdars%E2%80%93wcs-mess, Accessed on
[9] S. Licul, A. Petros and I. Zafar, "Reviewing SDARS Antenna Requirements", Available at: https://www.mwrf.com/markets/reviewing-sdars-antenna-requirements.
[10] N. Haller, "Mobile Antennas for Reception of S-DARS", *Proceedings of IEEE International Symposium on IEEE Antennas and Propagation Society*, pp. 426-429, 2001.
[11] R.A. Burberry, "*VHF and UHF Antennas*", The Institution of Engineering and Technology, 1992.
[12] B.D. Hart, "*Single Sideband Systems and Circuits*", 2nd Edition, McGraw-Hill, 1995.
[13] I. Hunter, R. Ranson, A. Guyette and A. Abunjaileh, "Microwave Filter Design from a System Perspective", *IEEE Microwave Magazine*, Vol. 8, No. 5, pp. 71-77, 2007.
[14] P.I. Mak and D. Leenaerts, "Low-Noise Amplifier Design Techniques", *Proceedings of IEEE International Symposium on Radio Frequency Integrated Circuits*, pp. 1-5, 2014.
[15] C. Tan and A. Wong, "Using Pre-Filter LNA Modules to Improve Receiver Sensitivity during Simultaneous GPS Operation", Available at: https://www.rfglobalnet.com/doc/using-pre-filter-lna-modules-to-improve-recei-0001.
[16] R.G. Meyer and A.K. Wong, "Blocking and Desensitization in RF Amplifiers", *IEEE Journal of Solid-State Circuits*, Vol. 30, No. 8, pp. 944-946, 1995.
[17] M. Imtiaz, "New Integrated SDARS Antenna Element for Automotive Applications", Master Thesis, Faculty of Engineering and Sustainable Development, University of Gavle, 2011.
[18] A. Petros, R. Pla and Z. Imtiaz, "Antenna Measurement Techniques for SDARS Antennas", *Proceedings of International Conference on Antenna Measurement Technology*, pp. 322-327, 2004.
[19] D.W. Wu, J.S. Wei, C. Su, R.M. Parkhurst, S.L. Fu, S. Chang and R.B. Levitsky, "An Enhancement-Mode PHEMT for Single-Supply Power Amplifiers", *Proceedings of International Conference on Microwave*, pp. 1-7, 1999.
[20] Avago Technologies, "Development of E-pHEMT Technology", Available at: https://www.eeweb.com/profile/avago-technologies/articles/development-of-e-phemt-technology
[21] C.L. Lim, "0.5W High Linearity Power Amplifier for Broadband Wireless (3.3~3.9GHz)", *Proceedings of International Conference on Microwave*, pp. 1-5, 2007.
[22] C. L. Lim, "Balanced UHF LNA Simplifies Cell Towers", *Microwaves and RF*, Vol. 52, No. 9, pp. 1-5, 2013.
[23] C.L. Lim, "Compact LNA Drives 2.5-GHz Base Stations", *Microwaves and RF*, Vol. 53, No. 1, pp. 50-59, 2014.
[24] C.L. Lim, "Low-Noise Amplifier Aids TDD Small Cells", *Microwaves and RF*, Vol. 56, No. 7, pp. 44-48, 2017.
[25] C.L. Lim, "Setting New Noise Performance Benchmarks using Wideband Low-Noise High-Linearity LNAs", *Microwave Journal*, pp. 58-76, 2011.
[26] C.L. Lim, "LNA Lowers Noise, raises OIP3 at 3.5GHz", Microwaves and RF, Vol. 51, No. 2, pp. 11-18, 2011.
[27] R.C. Ruby, P. Bradley, Y. Oshmyansky, A. Chien and J.D. Larson, "Thin Film Bulk Wave Acoustic Resonators (FBAR) for Wireless Applications", *Proceedings of International Conference on Ultrasonics*, pp. 813-821, 2001.
[28] R. Ruby, "11E-2 Review and Comparison of Bulk Acoustic Wave FBAR, SMR Technology", *Proceedings of Ultrasonics Symopsium*, pp. 1-5, 2007.
[29] Avago Technologies, "FBAR Filters", Available: https://www.broadcom.com/products/wireless/fbar.
[30] Avago Datasheet, "ACPF-8140 Bandpass Filter for 3GPP band 40", Available at: https://www.broadcom.com/docs/docs/AV02-3746EN.
[31] Triquint Semiconductor, "885014 2332.5 MHz BAW filter", Available at: https://html.alldatasheet.vn/html-pdf/683482/TRIQUINT/885014/383/1/885014.html
[32] Rogers Corporation, "RO4000 Series High Frequency Circuit Materials", Available at: https://www.rogerscorp.com/documents/726/acs/RO4000-LaminatesData-Sheet.pdf
[33] W. Domino, N. Vakilian and D. Agahi, "Polynomial Model of Blocker Effects of LNA/Mixer Devices", *Applied Microwave and Wireless*, Vol. 6, No. 1, pp. 30-44, 2001.
[34] J. Borremans, G. Mandal, V. Giannini, B. Debaillie, M. Ingels, T. Sano, B. Verbruggen and J. Craninckx, "A 40nm CMOS 0.4-6GHz Receiver Resilient to Out-of-Band Blockers", *IEEE Journal of Solid-State Circuits*, Vol. 46, No. 7, pp. 1659-1671, 2011.
[35] A. Mirzaei, H. Darabi, A. Yazdi, Z. Zhou, E. Chang and P. Suri, "A 65nm CMOS Quad-Band SAW-Less Receiver SoC for GSM/GPRS/EDGE", *IEEE Journal of Solid-State Circuits*, Vol. 46, No. 4, pp.1-15, 2011.
[36] C.Y. Yu, I. Lu, Y.H. Chen, L.C. Cho, C. Sun, C.C. Tang, H.H. Chang, W.C. Lee, S.J. Huang, T.H. Wu, C.S. Chiu and G. Chien, "A SAW-less GSM/GPRS/EDGE Receiver Embedded in 65-nm SoC," *IEEE Journal of Solid-State Circuits*, Vol. 46, No. 12, pp. 3047-3060, 2011.
[37] D. Murphy, H. Darabi, A. Abidi, A.A. Hafez, A. Mirzaei, M. Mikhemar and M.F. Chang, "A Blocker-Tolerant, Noise-Cancelling Receiver", *IEEE Journal of Solid-State Circuits*, Vol. 47, No. 12, pp. 1234-1242, 2012.
[38] I. Fabiano, M. Sosio, A. Liscidini and R. Castello, "SAW-Less Analog Front-End Receivers for TDD and FDD", *Proceedings of International Conference on Solid State Circuit*, pp. 1138-1145, 2013.
[39] R. Marino and A. Fuchs, "Dual Antenna System for Mobile SDARS Application", Technical Paper, SAE International, pp. 1-8, 2001.
[40] Q. Xue, H. Wong, K.M. Shum, K.M. Luk and C.H. Chan, "Active Receiving Antennas for Automotive Applications", *Proceedings of International Symposium on Antennas and Propagation*, pp. 20-25, 2004.
[41] California Eastern Laboratories Datasheet, "UPG2310TK GaAs MMIC Low Noise Amplifier for Satellite Radio", Available at: http://www.cel.com:8080/parts.do?command=loadandidRootPart=730
[42] M.S. Sharawi and D.N. Aloi, "A Compact Dual-Band RF Front-End and Board Design for Vehicular Platforms",

International Journal of Electronics, Vol. 99, No. 3, pp. 333-349, 2012.

[43] Y.P. Hong, J.M. Kim, S.C. Jeong, D.H. Kim, M.H. Choi, Y. Lee and J.G. Yook, "S-band Dual-Path Dual-Polarized Antenna System for Satellite Digital Audio Radio Service (SDARS) Application", *IEEE Transactions on Microwave Theory and Techniques*, Vol. 54, No. 4, pp. 1569-1575, 2006.

[44] T. Schwingshackl, "BFP740/BFP640 series 2 Stage LNA for 2.330GHz SDARS", Available at: www.infineon.com, Accessed on 2010.

[45] AN11066 NXP Application Note, "SDARS Active Antenna 1st Stage LNA with BFU730F, 2.33GHz", Available at: https://www.nxp.com/docs/en/application-note/AN11066.pdf.

[46] Skyworks, "SKY67175-306LF: 2320-2345MHz Two-Stage, High Gain Low-Noise Amplifier", Available at: http://www.skyworksinc.com/uploads/documents/SKY67175_306LF_202684C.pdf.

APPENDIX

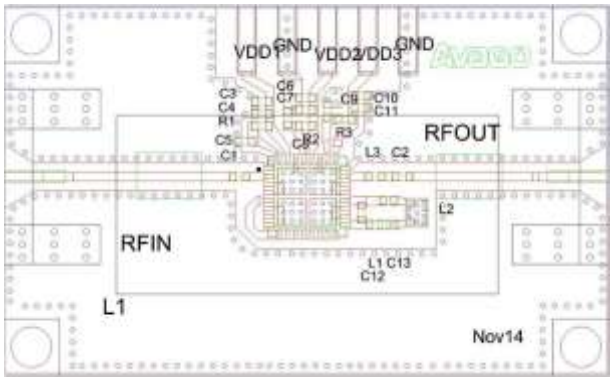

Fig.15. Part placement diagram for evaluation fixture

Table.4. Evaluation fixture's bill of material

#	Value	Part No	size	Vendor
L1	9.1 nH	-	201	-
L2		885014	-	Triquint
L3	1nH	LQG15HS1N0S02	402	Murata
C1	3.3pF	GJM1555C1H3R3CB01D	402	Murata
C2	100pF	GRM1555C1H101JD01E	402	Murata
C3	-	-	-	-
C4	4.7uF	GRM155R60J475ME760	402	Murata
C5	4.7uF	GRM155R60J475ME760	402	Murata
C6	-	-	-	-
C7	4.7uF	GRM155R60J475ME760	402	Murata
C8	4.7uF	GRM155R60J475ME760	402	Murata
C9	4.7uF	GRM155R60J475ME760	402	Murata
C10	-	-	-	-
C11	4.7uF	GRM155R60J475ME760	402	Murata
C12	-	-		
C13	0.4 pF		201	
JU	0 R		201	
R1	6.2kohm	RMC1/16S-622JTH	402	Kamaya
R2	24kohm	RMC1/16S-243JTH	402	Kamaya
R3	5.1kohm	RMC1/16S-512JTH	402	Kamaya